Dijlah J. Agric. Sci.، 5 (3): 61-80, 2026

Dijlah Journal of Agricultural Sciences
Journal homepage: https://djas.uowasit.edu.iq/index.php/djas/en

Research article

Spatiotemporal Variability of Physicochemical Water Quality Parameters in the Tigris River within Kut City, Iraq

Asawer Aad Yasser[1] and Rasha Mohan Salman [2]

[1,2] Department of Biology, College of Education for Pure Sciences, Wasit University, Wasit 52001, Iraq

ARTICLE INFO

Keywords:
Water Quality Index; Spatiotemporal Variation; Principal Component Analysis; Tigris River; Organic Pollution; Semi-arid Watershed

Article history:
Received: 18 May 2026
Accepted: 23 Jun 2026
Online: 30 Jun 2026

ABSTRACT

This study examined the spatiotemporal variations of water quality of Tigris River in Al-Kut city, Iraq to evaluate anthropogenic and hydrological effects. Sixteen physicochemical parameters were analysed from September 2025 to May 2026 and sampled monthly at four monitoring stations, according to the ISO 5667 protocols. The results showed stable baseline levels of pH (7.27±0.19) and dissolved oxygen (8.08±1.66mg/L); while pollution indicators (COD, phosphate, turbidity and nitrate) exhibited high variability (CV>70%). A distinct spatial gradient was observed, with the upstream site being optimal and sites in the urban areas being extremely degraded. Progressive deterioration was found from the autumn (WQI ≈ 50) to the spring (WQI >1300) with seasonal analysis; this was attributed to the lack of hydrological flushing and thermal changes, and possible cumulative organic loadings. Two independent drivers were found using principal component analysis: mineral concentration/dilution gradient (PC1, 51.6% variance) and an organic/nutrient enrichment axis (PC2, 19.6%). Water quality patterns were also confirmed by hierarchical clustering which showed that spatial differentiation is completely masked by the effect of seasonal forcing. These results emphasize the importance of the system during the spring season and the need for a system of seasonally adjusted management practices to lessen the effects of urban and agricultural pollution in semi-arid watersheds.

1. Introduction

River ecosystems are an integral component of global water cycle. Apart from supporting human societies and the natural environments, these river systems serve as areas where potable water is available as one of its major functions, and also serve as habitats for aquatic and riparian biota and as areas of agricultural irrigation, in addition to industrial uses (Ighalo & Adeniyi, 2021). Rivers shall also be indirectly useful, and have significant roles in moving sediments and nutrients, and in controlling biogeochemical cycles, within healthy connected ecosystems. But the anthropogenic pressures are increasing and leading to the degradation of river water quality and this is still a threat to all types of ecological integrity and human well-being (Candraningtyas et al., 2026).

*Corresponding author:
std.2024205.a.yasir@uowasit.edu.iq (Asawer Aad Yasser)

2790 – 5985/©Wasit University College of Agriculture

The stress on surface water bodies is unprecedented as a result of the discharges of different point and nonpoint sources, mostly domestic sewage sewage, industrial effluents, and agro-chemicals carried by runoff (Wetzel, 2001). These anthropogenic activities cause widespread alterations of the physical, chemical and biological properties of the waters, making them unsuitable for most human uses. Aquatic ecosystems from an ecological point of view are very sensitive to even minor changes in the balance of their biological communities (Chapman, 1996).

Therefore, the present study is intended to provide light on the various aspects of river water pollution with particular emphasis on the sources of river water pollution and the extent of its effects on the environment (Kuchangi et al., 2023). The chapter is an integrated overview of surface water with a special section on river ecology and its values and problems of pollution. The literature includes details on the surface water pollution, the primary sources of the pollution and the additional impact of the wastewater discharge on the water quality of a river (Fernandes, 2023). Microbial indicators have special significance as they give information about the probability of contamination from faecal origin and the potential hazard of the microorganisms to humans, e.g. Escherichia coli and coliform bacteria (Paruch & Mæhlum, 2012).

This study aimed to study the temporal and spatial fluctuations of physical, chemical water quality parameters in Tigris River in Al-Kut City, Iraq and to assess the impacts of human activities and seasonal hydrological changes on water quality in the river. The study analyzed monthly monitoring data from four sampling stations in the study area from September 2025 to May 2026, to determine water pollution gradients, seasonal water quality deterioration trends and key environmental factors influencing water quality. This research is important because it helps to understand the interaction between urban discharge, agricultural runoff, and seasonal flow reduction on river ecosystem health in a semi-arid climate. Findings are of critical importance for the effective formulation of water management strategies adapted to the seasons, formulating pollution control policies, and supporting sustainable freshwater resource management for Iraq and similar watersheds.

2 .Materials and Methods

2.1 .Study Area and Sampling Design

This study was carried out in Al-Kut city in Wasit Governorate in the southeast of Baghdad city, Iraq, about 180 km from Baghdad city. Al-Kut has a semi-arid climate and is an important hydrological and urban center where the Tigris flows. The river is the main source of freshwater for the domestic, agricultural and ecological needs in the region. The river system faces several environmental stresses from rising urbanisation, agricultural uses and wastewater release which can affect water quality and ecosystem health.

The 4 survey sites, the monitoring stations were chosen due to their hydrological significance, anthropogenic influence, accessibility and in direct relation with the Tigris River system. To show the spatial differences in physicochemical and pollution parameters, the selected stations were from different environmental and urban conditions of Al-Kut City. These sampling stations were: Station 1 (Al-Kut/Baghdad Checkpoint), Station 2 (Al-Ahdab Bridge), Station 3 (Al-Zahraa), and Station 4 (Al-Kardhiya). These sites include those impacted by urban run-off, home sewage, bridge related uses, and varying hydrological characteristics.

Water samples were taken according to internationally accepted scientific procedures and according to the guidelines of ISO 5667 for water quality sampling. The geographic coordinates and site description of the monitoring stations are provided in Table 1 and spatial distribution of sampling locations in Figure 1.

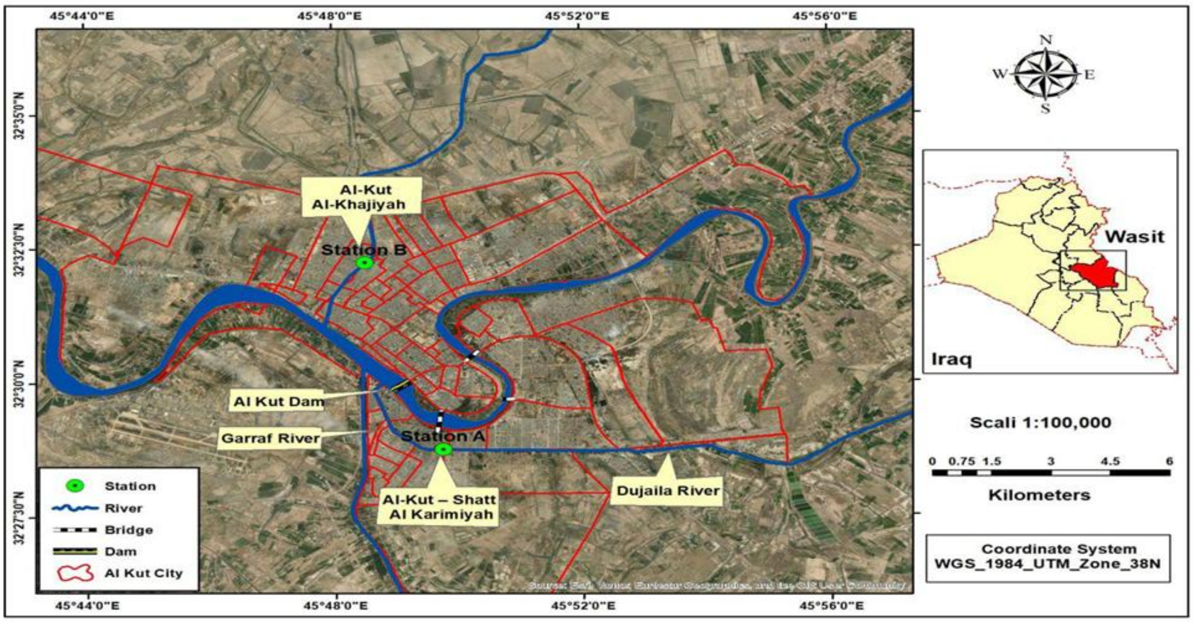

Figure 1: Map showing the research sites

Table 1: Monitoring Station Geographical Coordinates and Features

A	Area	X	Y
1	AL – Kut /Bagdad Checkpoint	45.72625	32.533613
2	AL – Ahdab Bridge	45.829959	32.490346
3	AL - Zahraa	45.833436	32.526189
4	AL - Kardhiya	45.948329	32.584088

2.2 .Sample Collection and Preservation

The four monitoring stations were sampled monthly from September, 2025 to May, 2026. All sampling was done in pre-cleaned polyethylene bottles, under standardized field conditions, to minimize and prevent contamination and analytical variation. Samples of surface water were taken from about 20-30cm from the surface of the water to prevent floating debris and surface films being sampled.

Samples for physicochemical analysis were preserved immediately after collection and transported to the laboratory in insulated ice containers at about 4°C and analyzed as soon as possible within the recommended holding time for the samples to ensure sample integrity. All measurements were duplicate to provide analytical precision and reliability.

2.3 .Physicochemical Analysis

The water samples from Tigris river were analyzed for physicochemical characteristics by standard methods for water and wastewater. The water parameters that were investigated were water temperature, pH, turbidity, electrical conductivity (EC), total dissolved solids (TDS), salinity, dissolved oxygen (DO), biochemical oxygen demand (BOD_5), chemical oxygen demand (COD), total hardness

(TH), calcium (Ca^{2+}), magnesium (Mg^{2+}), sulfate (SO_4^{2-}), chloride (Cl^-), nitrate (NO_3^-), and phosphate (PO_4^{3-}), and total alkalinity.

Portable digital water and pH meters were used to take measurements in the field. The electrical conductivity was measured with a conductivity meter (in µS/cm); the total dissolved solids were estimated from electrical conductivity measurements by reference to standard conversion relationships. Portable salinity meter was used for salinity measurements and reported in ppt (parts per thousand). The turbidity was measured by nephelometric turbidity meter and expressed in nephelometric turbidity unit (NTU).

The total hardness, calcium and magnesium content were determined under controlled conditions in the laboratory by titrimetric methods using ethylenediaminetetraacetic acid (EDTA). The concentrations of sulfate and chloride were estimated by spectrophotometric and argentometric methods respectively. This involved analysing nutrient parameters (such as nitrate and phosphate) with colourimetric methods. The total alkalinity was measured by acid titration with standard sulfuric acid solution. All analytical procedures were conducted using the internationally accepted standard methods to assure the accuracy, reproducibility and comparability of results.

2.4 .Statistical and Data Analysis

Physicochemical data from four monitoring stations sampled monthly between September 2025 and May 2026 were organized by station, month, and season (autumn, winter, and spring). Descriptive statistics, including mean, standard deviation, median, minimum, maximum, and coefficient of variation, were calculated for the 17 physicochemical parameters. Water Quality Index (WQI) was determined using the weighted arithmetic method to assess overall water quality. Pearson correlation analysis was applied to evaluate relationships among parameters, while principal component analysis (PCA) and hierarchical clustering analysis (HCA) were performed using standardized data to identify dominant pollution factors and sample-grouping patterns. Graphical outputs included heatmaps, PCA biplots, and dendrograms. Statistical analyses and visualizations were performed using pandas, NumPy, SciPy, scikit-learn, and Matplotlib.

3 .Results and Discussion

3.1 Descriptive variation of physicochemical parameters

The descriptive statistics of the 16 physicochemical parameters that were subjected to analysis, 36 samples in Tables 2 & 3. The overall mean pH value of the water remained stable and close to neutral during the period of the study (mean = 7.27 ± 0.19; range 7.0–7.7) with very little relative variability (CV = 2.61%). The dissolved oxygen (DO) concentration generally was adequate, with a mean of 8.08 ± 1.66 mg/L (CV = 20.59%), and the water temperature showed a normal level of seasonal fluctuations (mean = 18.86 ± 4.17°C; range: 11.0 – 27.5°C). The moderate variability (CV range: 20.5%–31.7%) in the parameters related to the ionic strength and hardness such as electrical conductivity (EC), total dissolved solids (TDS), salinity, total alkalinity, and total hardness of the study area indicated uniform geological and anthropogenic influences. Organic pollution and nutrient loading, on the other hand, exhibited much greater heterogeneities in their indicators. COD exhibited the highest variation (mean = 36.18 ± 41.39 mg/L; CV = 114.4%) followed by phosphate (PO_4; CV = 129.2%), turbidity (CV = 101.7%) and nitrate (NO_3; CV = 74.1%) indicating episodic point and non-point source inputs. There was also a large variation in biochemical oxygen demand (BOD_5); the mean BOD_5 was (mean = 4.43 ± 2.09 mg/L (CV = 47.1%) and the maximum values were close to those of organic enrichment.

Table 2. Descriptive statistics of physicochemical water quality parameters (n = 36)

Parameter	Count	Mean	SD	SE	Median	Minimum	Maximum	CV_percent
BOD5	36	4.428	2.087	0.348	4.75	1.1	9	47.134
COD	36	36.179	41.388	6.898	18	3	113	114.397
Ca^{2+}	36	119.792	34.01	5.668	130.5	67	210	28.391
Chloride	36	144.458	52.252	8.709	169	67	220	36.171
DO	36	8.075	1.662	0.277	7.85	6	11.3	20.586
EC	36	1349.083	378.278	63.046	1559	750	1795	28.04
Mg^{2+}	36	43.5	10.574	1.762	42.25	31	80	24.309
NO_3^-	36	2.127	1.577	0.263	2.65	0.1	5.13	74.138
PO_4^{3-}	36	3.632	4.691	0.782	2.125	0.02	16	129.178
SO_4^{2-}	36	336.875	97.105	16.184	379.75	190	450	28.825
Salinity	36	0.863	0.242	0.04	0.998	0.48	1.149	28.04
TDS	36	787.799	249.988	41.665	831	375	1108	31.733
Total_Alkalinity	36	186.958	40.005	6.668	195	128	280	21.398
Total_Hardness	36	472.458	96.929	16.155	514	320	600	20.516
Turbidity	36	95.782	97.401	16.233	66.25	3.51	305	101.69
Water_Temp	36	18.86	4.17	0.695	19.25	11	27.5	22.111
pH	36	7.267	0.19	0.032	7.2	7	7.7	2.612

These patterns highlight the dynamic nature of water quality in the study system: stable baseline water quality of key parameters is coupled with high spatiotemporal variability of pollution sensitive parameters.

Table 3. Spatial variation of physicochemical parameters among the four sampling stations

Parameter	**Unit**	**St1 Mean ± SD**	**St2 Mean ± SD**	**St3 Mean ± SD**	**St4 Mean ± SD**
Water temperature	°C	18.23 ± 5.90	18.95 ± 3.75	18.88 ± 3.66	19.37 ± 3.62
Turbidity	NTU	52.43 ± 53.19	130.51 ± 131.25	104.48 ± 108.50	95.70 ± 78.24
TDS	mg/L	743.19 ± 269.20	808.58 ± 257.99	812.42 ± 255.86	787.00 ± 255.97

EC	µS/cm	1257.83 ± 372.99	1404.00 ± 394.89	1392.67 ± 410.36	1341.83 ± 384.23
pH	pH unit	7.14 ± 0.06	7.22 ± 0.12	7.52 ± 0.12	7.18 ± 0.16
DO	mg/L	9.98 ± 1.29	6.77 ± 0.63	6.72 ± 0.52	8.83 ± 1.00
BOD_5	mg/L	2.05 ± 0.54	5.49 ± 0.71	5.63 ± 0.66	4.53 ± 2.92
COD	mg/L	9.47 ± 3.14	45.40 ± 45.79	45.27 ± 45.79	44.58 ± 47.12
Total hardness	mg/L as $CaCO_3$	473.83 ± 86.88	483.83 ± 110.49	470.83 ± 109.54	461.33 ± 95.18
Ca^{2+}	mg/L	113.67 ± 25.11	132.33 ± 44.65	115.67 ± 36.37	117.50 ± 29.48
Mg^{2+}	mg/L	47.50 ± 17.69	41.50 ± 8.54	42.00 ± 4.76	43.00 ± 7.44
SO_4^{2-}	mg/L	324.83 ± 101.07	353.00 ± 96.62	336.83 ± 103.78	332.83 ± 102.26
Chloride	mg/L	129.83 ± 46.19	152.00 ± 54.83	153.67 ± 60.33	142.33 ± 52.54
Total alkalinity	mg/L as $CaCO_3$	172.33 ± 26.05	208.67 ± 51.92	190.83 ± 39.84	176.00 ± 33.42
PO_4^{3-}	mg/L	1.02 ± 0.98	4.94 ± 4.30	5.68 ± 7.42	2.88 ± 2.63
NO_3^-	mg/L	1.30 ± 1.46	2.42 ± 1.46	2.79 ± 1.95	2.00 ± 1.21
Salinity	ppt	0.81 ± 0.24	0.90 ± 0.25	0.89 ± 0.26	0.86 ± 0.25

3.2 Spatial variation among sampling stations

Water Quality Index (WQI) distribution was shown on the four sampling stations in Figure 2. The mean WQI values also showed significant spatial variability in WQI at the stations ranging from about 225 at St1 to 975 at St3. The mean water quality index (WQI) for station 1 (St1) was lowest at 225 ± 175, suggesting relatively good water quality at this station. The means of WQI values at stations 2 and 3 were quite high (900 ± 675 and 975 ± 1000, respectively) indicating relatively poor water quality at both of these stations. The intermediate conditions were in Station 4, the mean WQI in the station was ~575 ± 425.

The amount of variability around mean values (error bars) was very high, especially for St3 (0 to 2000), compared to St2 (250 to 1575). The variability is high suggesting significant temporal variability in water quality parameters at these stations, which may be attributed to seasonal effects, changing pollution input, or episodic pollution events. St1 had the widest range of water quality conditions as well as the highest variability range. The great spatial variation, with St1 having the highest performance and St3 the lowest, indicates anthropogenic pressures are not evenly distributed throughout the study area or that there are different pollution sources.

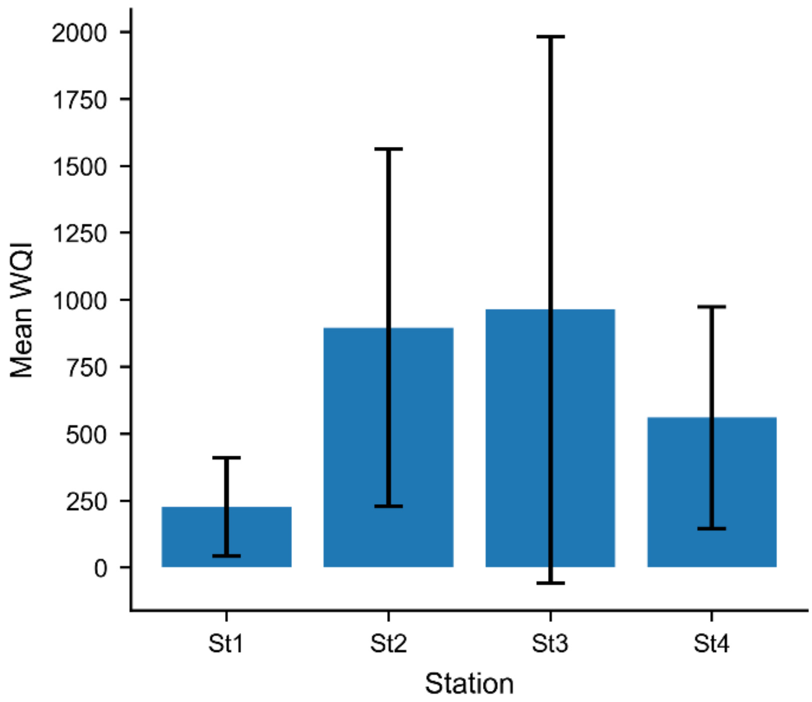

Figure 2. Mean WQI values by sampling station of which error bars indicate standard deviation, reflecting temporal variation in the water-quality status at each station.

3.3 Monthly and seasonal variation

The monthly variations of the main physicochemical parameters are shown in the four sampling stations of Figure 3. The water temperature had a distinct annual cycle with a peak in September–October (23–28°C), a sharp decrease during the cooler months (December–February; 11–15°C), and a gradual recovery from March onwards. Dissolved oxygen (DO) showed an opposite trend, with maximum values from December to February (9.0–11.5 mg/L) and decreasing values with higher temperatures. Stations 1 consistently had the highest DO concentrations during the monitoring period whereas Stations 2 – 4 had more variability in DO concentrations from month to month.

The temporal trend for electrical conductivity (EC) and total dissolved solids (TDS) were almost identical with increased concentrations in September to February (EC: 1400–1800 μS/cm and TDS: 1000–1100 mg/L) and a sharp drop in concentrations beginning in March, with a plateau at lower levels through May (EC: 750–900 μS/cm and TDS: 400–500 mg/L). Lowest EC and TDS values were recorded at station 1 for all the months indicating that this site might have a lower ionic loading or higher dilution capacity.

Turbidity was relatively low throughout the autumn season (September–November; >30 NTU) and significantly higher in the winter (December–February) with both stations 2 and 3 reaching values of around 300 NTU. Comparatively, the turbidity of Station 1 was relatively low with minimal fluctuations, and was seldom higher than 120 NTU. The temporal escalations were different for the organic and nutrient indicators. Biochemical oxygen demand (BOD_5) was fairly consistent in most stations (2–6 mg/L) except for a distinct mid-winter peak at Station 4 (up to 9 mg/L). The concentrations of chemical oxygen demand (COD) and nitrate (NO_3^-) were low in the autumn and early winter but rose sharply in March. By May, COD levels at all stations surpassed 100 mg/L, while NO_3^- levels were 4–5 mg/L, with Station 3 having the highest nitrate concentrations. All of these pollution-sensitive parameters were consistently found to be the lowest at Station 1 during the study period.

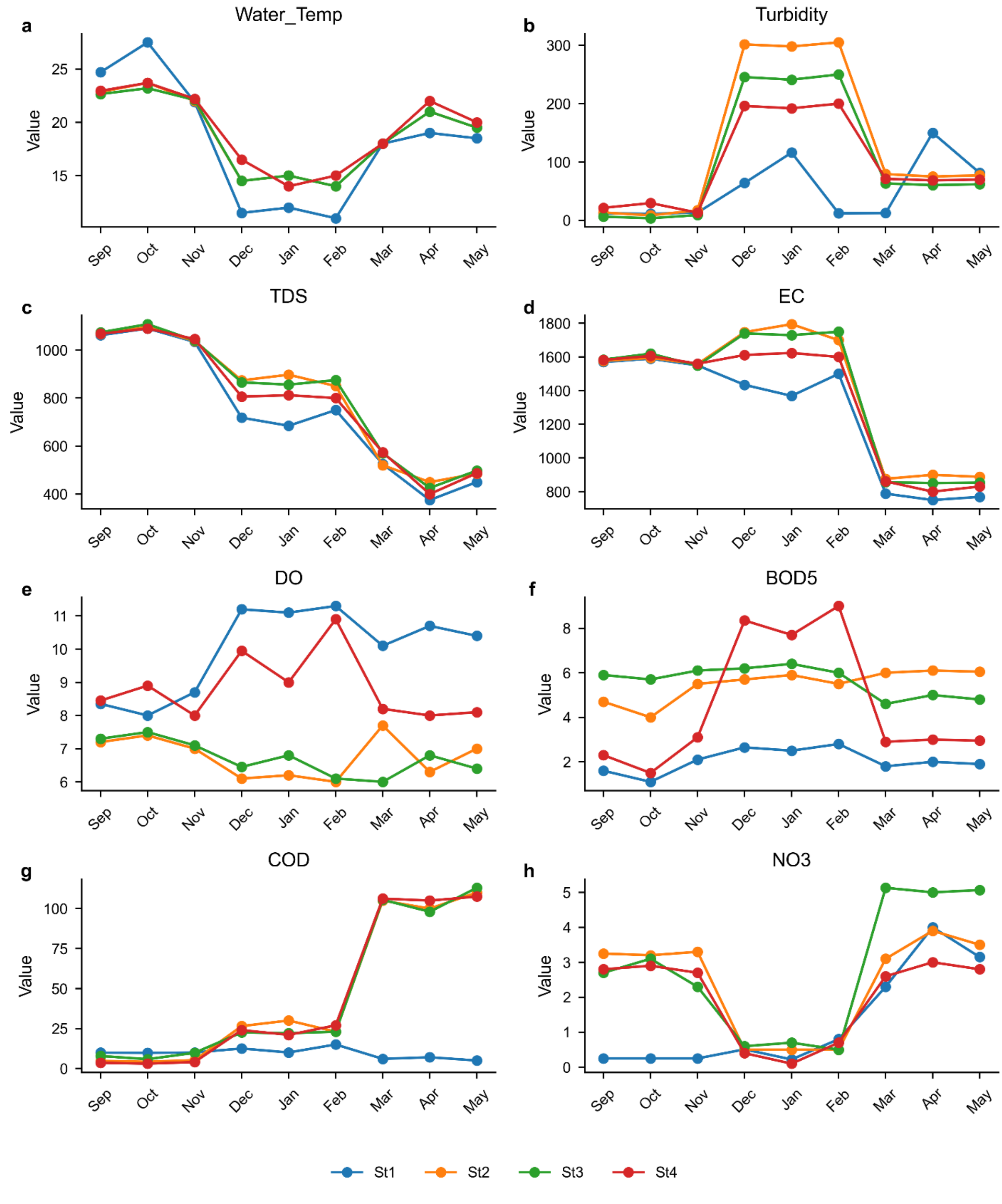

Figure 3. Monthly trends of selected key physicochemical parameters measured at the four stations (a. water temperature, b. turbidity, c. TDS, d. EC, e. DO, f. BOD_5, g. COD, and h. nitrate).

Seasonal distribution of the Water Quality Index (WQI), with a clear and increasingly large drop in water quality from autumn to spring in Figure 4. WQI values were generally low and close together in the autumn, with both the mean (green triangle) and the median (orange line) being close to 50.

The small interquartile range and short whiskers show low spatial and temporal variability, which suggests a relatively constant and good water quality in this time period.

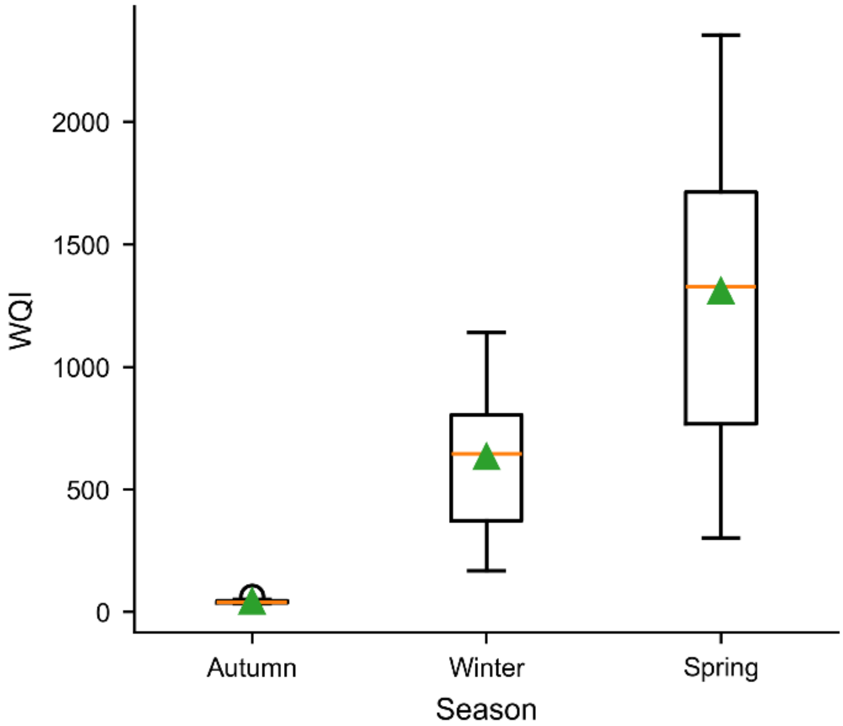

Figure 4. Seasonal distribution of WQI values across the study period. The boxplots compare water-quality variability among autumn, winter, and spring seasons.

During the winter, WQI rose significantly, with the majority (central 50%) of observations ranging between about 200 and 850. With the mean and median near 600-650, the extended whiskers (~150 to ~1150) show increasing sample variation. This transition may indicate a transition to cumulative stressors, possibly related to more restricted flow regimes, changing mixing regimes or greater anthropogenic loads in the cooler months.

The highest WQI values were observed in the spring season with the interquartile range significantly increased to around 750–1700 and the mean and median ranging between 1300–1350. There was some spatiotemporal variability and episodic water quality excursions at some stations, with the spring distribution having the widest overall range (~300 to >2300). Mean and median markers are consistent across seasons with little distributional skewness, further supporting the reliability of seasonal gradient observed.

These results together show a clear seasonal increase in the WQI, whereby water quality moves from good/excellent in the autumn to poor/very poor in spring. This trend may have been caused by seasonal hydrological variations (such as less dilution in low flow conditions), biogeochemical effects related to temperature, and a progressive effect by the point and non-point pollution sources throughout the monitoring period.

3.4 Water Quality Index assessment

The Water Quality Index (WQI) for the four monitoring stations are shown in Figure 5 as they change over time and space. The WQI values were found to be uniformly low during autumn season (September-November) and were maintained within 50-100 indicating consistently good water quality with a limited spatial variability. In December, when stations 2, 3, and 4 a dramatic split occurred with 3 stations showing significant improvements in WQI values (around 1100, 600 and 650 respectively), and 1 station showing much lower values (~200). WQI trends from January to February were either levelled off or slightly dampened at Stations 2–4 while Station 1 experienced a steady rise. Spring (March-May) was the most impacted season in terms of water quality. The WQI values were the highest at Station 3 with a maximum of ~2,300 in March and continuing above 2,200 until May. At Station 2, the increase was similar, stopping at about 1550, and Station 4 had a slight increase from 800 to 1100. The increase was the least for Station 1, reaching ~550 in April, but there was a slight decrease in May. These trends show a seasonal increase in WQI, with spring being the most vulnerable season for water quality decline. Spatial ranking for each month is consistent, with the same ranking of (St3> St2> St4 >St1), indicating that these differences in pollution loading, hydrological regime or catchment characteristics do not diminish in time.

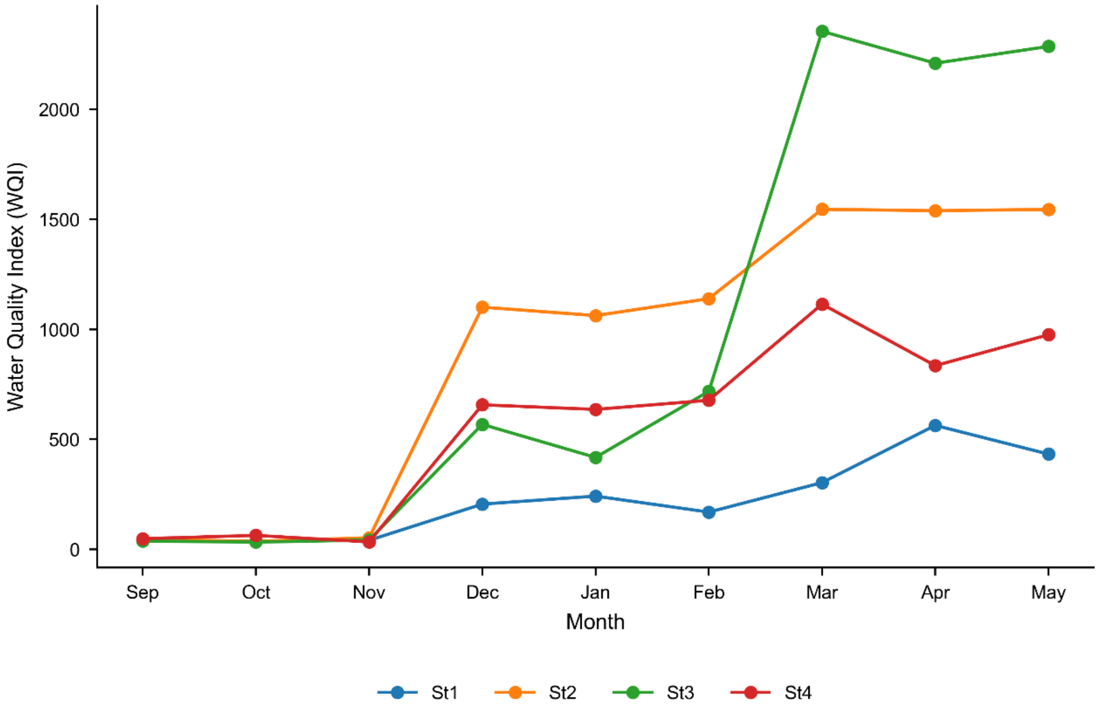

Figure 5. Spatiotemporal variation of the Water Quality Index (WQI) in Tigris River water within Kut city during the study period, trend lines compare monthly changes among the four sampling stations.

The Water Quality Index (WQI) for the four monitoring stations, September to May in Figure 6. For the autumn period (September–November), all of the sites had low WQIs that were fairly evenly distributed, ranging from 33.1 to 63.4, and reflecting consistently good water quality. In December, there was a large difference as Stations 2, 3 and 4 had high WQI values ranging from (568.2 to 1,193.8), while Station 1 had low values in the range of (169.4 to 303.4) and still had low values in the winter months (December–February).

The worst water quality was observed in spring (March-May) when the WQI rose significantly at all stations except St1. The degradation was the highest at Station 3, reaching a maximum of 2,355.2 in March and remaining high (2,210.3–2,286.6) until May. The trend at Station 2 was comparable with high concentrations (~1,540–1,546), while moderate (835.3–1,114.9) increases were recorded at Station 4. The growth was slowest at Station 1, with a maximum of 563.7 in April followed by a small decrease. The spatial hierarchy remained consistent throughout monitoring (St3 > St2 > St4 > St1), suggesting that there was a consistent spatial gradient in pollution loads, catchment influence, or hydrological flushing capacity. The heatmap shows that generally water quality conditions were low during the autumn season and greatly improved in late spring, especially at Stations 2 and 3.

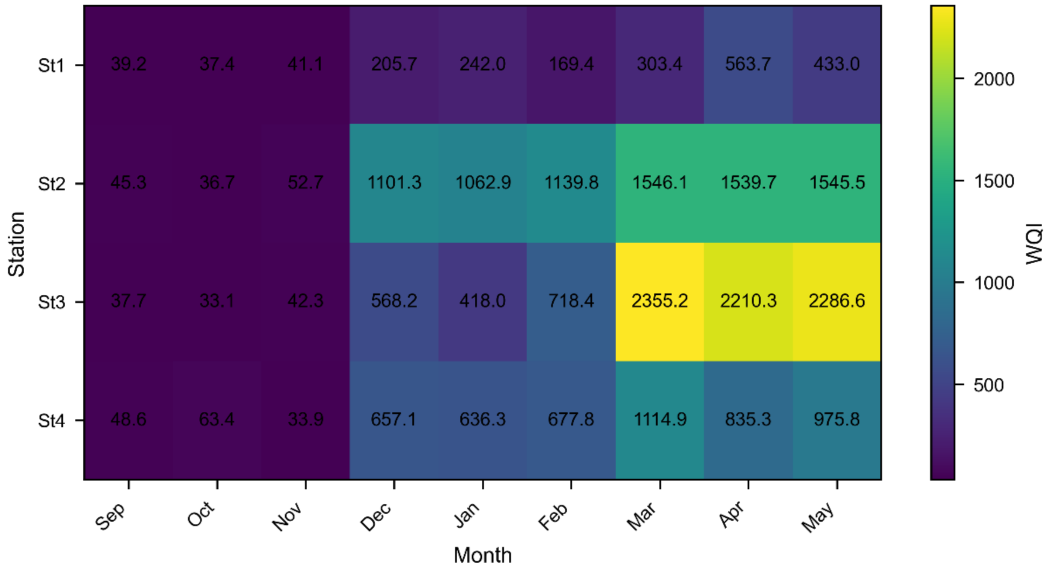

Figure 6. Representation of WQI values across stations and months among highlights periods and locations associated with relatively better or poorer water-quality conditions.

3.5 Correlation analysis

Inter-parameter relationship, identification of underlying hydrochemical processes and subsequent multivariate modeling were achieved through the use of Pearson correlation analysis (Figure 7). The correlation matrix outlines three different patterns of relationships:

1 .Strong Positive Associations (Ionic/Mineral Cluster)

Highly coherent positive correlation block ($r \approx 0.6 – 0.9$) was found between Ca^{2+}, Mg^{2}, Cl^{-}, SO_4^{2-}, EC, TDS, salinity and total hardness. The correlation between these variables is very close, suggesting that the same geochemical weathering processes or common anthropogenic sources of dissolved ions are affecting the water column, such as agricultural drainage, domestic wastewater or industrial effluents.

2 .Organic and Nutrient Coupling.

A strong positive correlation was found between BOD_5 and COD, which is indicative of a similar origin, the biodegradable organic matter loading and total organic matter loading. Some moderate correlation was observed between COD and PO_4^{3-}, indicating that there was concurrent enrichment of organic carbon and phosphorus, probably from sewage or agriculture runoff. In contrast, Nitrate (NO_3^{-}) had weak-to-negative correlations with the mineral ion cluster, yet it had positive correlations with PO_4^{3} and COD, suggesting a unique nitrogen-phosphorus-carbon nutrient pathway.

3 .Inverse Relationships (DO vs. Temperature and Organics)

Water temperature and organic indicators (COD and BOD_5) showed significant negative correlation with dissolved oxygen (DO). This inverse relationship is related to two well-known mechanisms: (i) less oxygen can be dissolved at higher temperatures and (ii) more oxygen is consumed by microbes in the breakdown of organic contaminants. These negative correlations are strong enough to indicate that DO is an important response variable to thermal and organic stress.

4 .Weakly Correlated Parameters

pH and turbidity were the least strongly correlated with most other variables (|r| < 0.4) and appear to be influenced by individual pollution suites other than those of the dominant pollutants described above, such as buffering capacity, sediment resuspension or localized erosion.

Synthesis for Multivariate Analysis.

The correlation structure effectively separates the data into two main pollution suites, (i) a mineral/ionic enrichment suite, depending on solute loading, and (ii) an organic/nutrient loading suite, inversely coupled with DO. These relationships are used to validate the removal of redundant variables to reduce dimensionality and give a statistical basis for the subsequent Principal Component and Cluster Analyses.

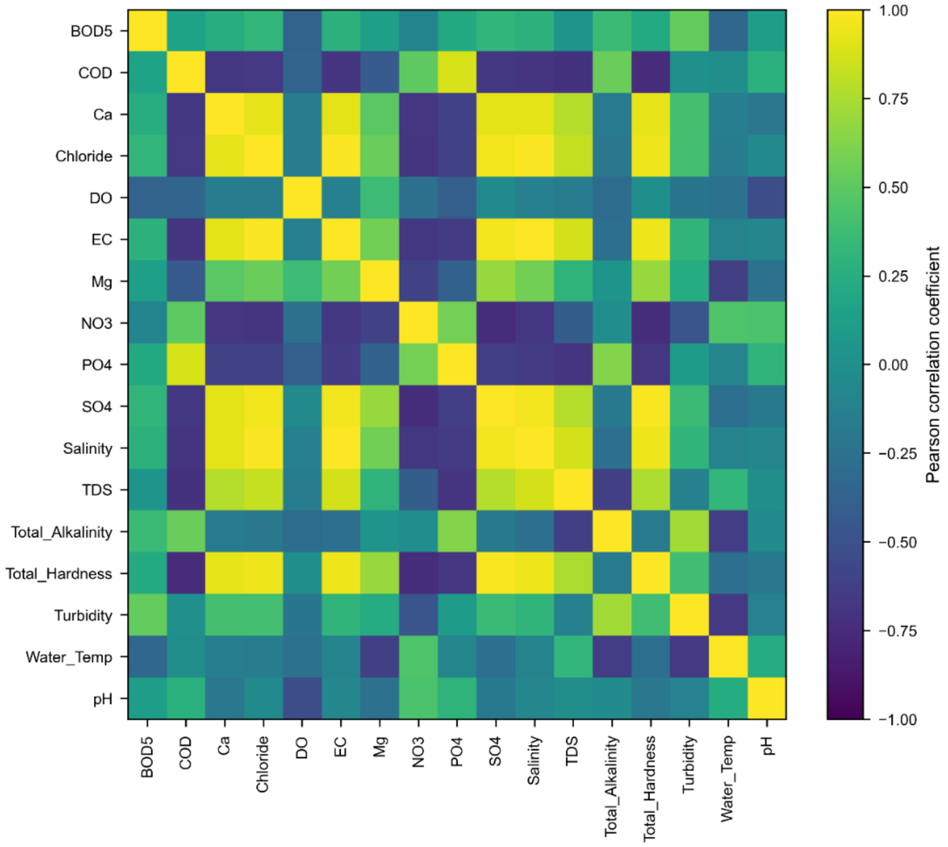

Figure 7. Pearson correlation heatmap of the measured physicochemical parameters of potential associations among salinity-related variables, organic pollution indicators, nutrients, and oxygen-related parameters.

3.6 Principal component analysis

The 16 physicochemical variables were reduced to fewer components using Principal Component Analysis (PCA) and the underlying variables (or drivers) identified. The first two principal components (PC1 and PC2) accounted for 71.2% of the total variance with PC1 explaining 51.6% and PC2 19.6% (Figure 8).

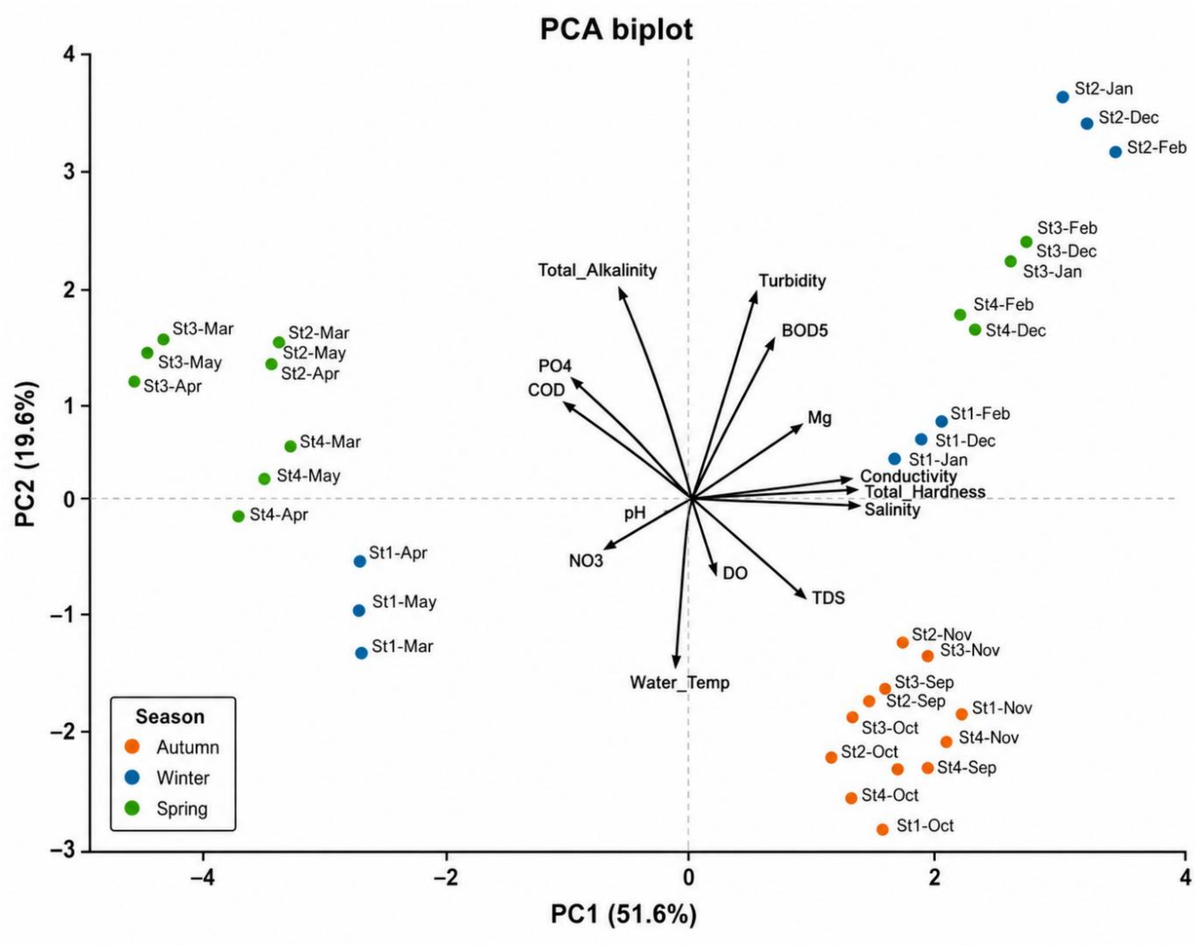

Figure 8. PCA biplot of physicochemical parameters and station-month samples

Electrical conductivity (EC), total dissolved solids (TDS), salinity, total hardness, Ca^{2+}, Mg^{2+}, Cl^{-} and SO_4^{2-} had positive strong loadings with PC1 (51.6% variance). The axis is mainly composed of a hadrochemical concentration/dilution gradient associated with seasonal variations in flow regime, evaporation and geogenic weathering. Those samples that fall on the positive side of the PC1 are high in ionic strength and mineral content, while negative PC1 scores are representative of low ionic strengths.

The positive relationships of PC2 (19.6% variance) with BOD, COD, PO_4^{3-}, turbidity, and total alkalinity, and the negative relationship of PC2 with water temperature and NO_3^{-}, indicated variance contributions. Higher variance contributions were indicated by the positive relationships of, turbidity, and total alkalinity, and the negative relationship of PC2 with water temperature and NO_3^{-}. This component picks up an organic/nutrient enrichment axis separate from the mineral baseline, and encompasses microbial decomposition, sediment resuspension, as well as agricultural and domestic nutrient inputs.

Sample distribution across the biplot reveals distinct seasonal and station-specific clustering:

The samples collected in the autumn period (September-November) is grouped together in the lower right quadrant (positive PC1, negative PC2), (high concentrations of background mineral loading, low concentrations of organic and nutrient loading), reflecting relatively high background mineral concentrations and low organic and nutrient loadings, which is indicative of relatively low anthropogenic stress and stable hydrological conditions.

Samples collected in the winter (Dec–Feb) fall into the upper right quadrant (positive PC1 and PC2), where concurrent increases in dissolved solids and organic and nutrient pollutants occurred. The alignment seems to indicate that flushing from the water is less, that point-source discharges are greater, and that biodegradable material has begun to build up, quite early.

Spring (Mar-May) samples are characterized as having severe decreases in EC, TDS and hardness (which may be due to higher runoff/dilution), and higher water temperatures and NO^{-} concentrations, and are displayed on the left side (PC1) of the plot.Samples from spring (Mar-May) are characterized as having dominant decreases in EC, TDS and hardness (likely due to increased runoff/dilution), and increases in water temperature and NO^{-} concentrations, and are displayed on the left side (PC1) of the plot. The stations with the highest WQI values and the highest pollution sensitivity (Stations 2 and 3) have the most extreme winter-to-spring trajectories.

The orthogonal separation of PC1 and PC2 confirm that there are two processes regulating water quality variability in the study system: (i) a seasonal hydrological control on baseline ionic/mineral concentrations, and (ii) an episodic organic/nutrient enrichment that is unrelated to temperature and nitrate regimes. These results confirm the correlation structure and the trends analyses at the monthly level, thus forming a powerful reduced dimensional framework for the hierarchical clustering of the analysed samples.

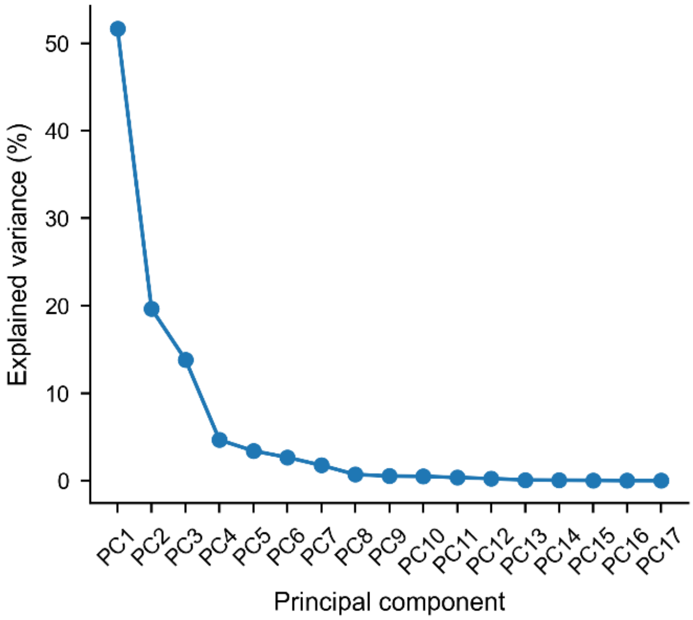

Figure 9. PCA scree plot showing cumulative variance of water quality parameters

Scree plot showing variance explained by all the extracted principal components (Figure 9). PC1 accounted for the highest percentage of variance (51.6%) followed by PC2 (19.6%) and PC3 (~14.0%). Together, the first three components accounted for the vast majority of data information (85.2%). A clear "elbow" is seen after PC3 where the curve levels off rapidly with successive components accounting for less than 5% of the variance. First three components were retained based on this visual threshold and Kaiser criterion (eigenvalue >1) for further analysis. The high amount of explained variance (71.2%) of PC1 and PC2 gives a firm and noise-filtered base to the biplot interpretation and allows the main hydrochemical gradients to be easily captured with as little as possible in the dimension reduction sense.

3.7 Cluster analysis

By hierarchical clustering using Euclidean distance, the samples from each station month showed a clear seasonal structure that was more important than spatial differentiation (Figure 10). The dendrogram shows a major split at the high linkage (about 25), which clearly divides the data into two large superclusters. The left branch shows all of the spring samples (March–May) grouped together at each of the four stations, suggesting a high degree of hydrochemical uniformity during this time despite the differences in background chemistry at each station. All samples in the fall and winter (September - February) are included in the right branch, and then divided into two distinct subgroups: early fall (September-November), and late fall/winter (December-February). In the seasonal clusters, the inter-sample Euclidean distances are consistently low (<6), meaning that the water quality profiles are very similar across the stations in each cluster at a given point of time.

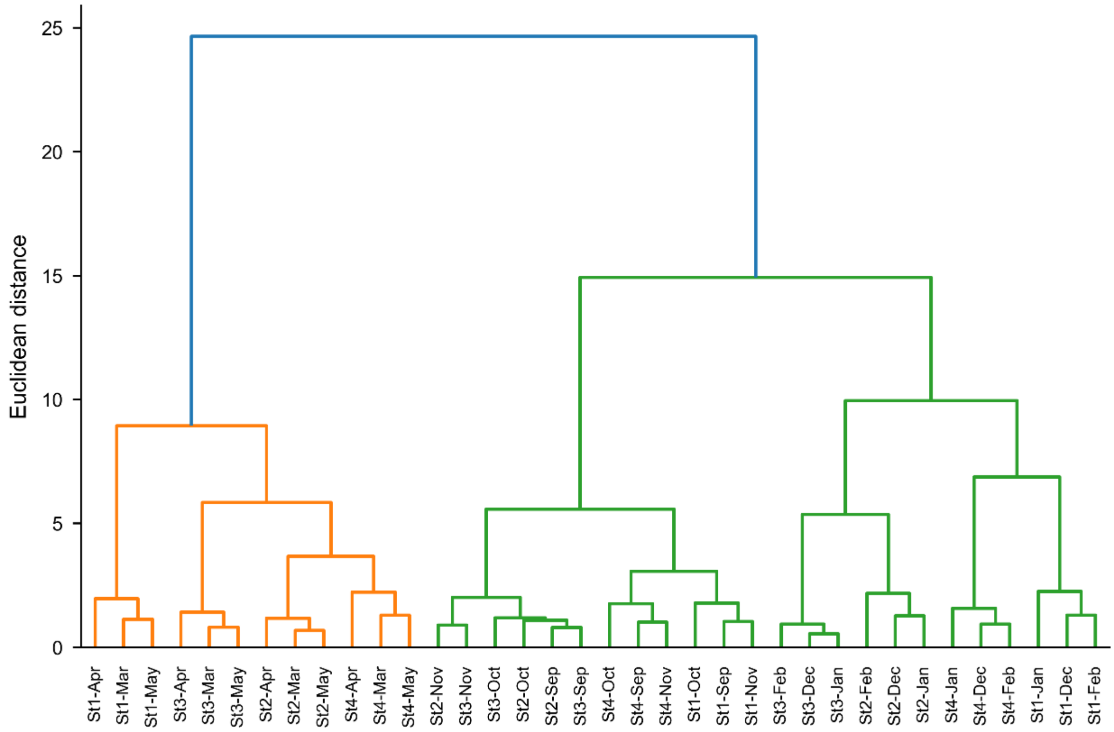

Figure 10. Hierarchical clustering dendrogram showing seasonal structuring of station-month water-quality profiles.

Notably, the primary clustering pattern is not correlated to sampling station, but rather seasonality, indicating that regional hydrological variation, temperature-driven biogeochemical processes and seasonally induced pollution loadings are more important to the overall water quality dynamics than localized spatial variation. This seasonal coherence very strongly supports the WQI temporal trajectories and PCA sample distributions, which validate that water quality degradation/recovery is predictable and system-wide, and cycles on an annual basis.

4.1 Spatial and seasonal water-quality changes

Seasonal hydroclimatic variations are the major controlling factors on the hydrochemical characteristics of Tigris River in Al-Kut City, while local spatial factors are less significant. Overall, a spatial hierarchy was found throughout the monitoring period (St1 < St4 < St2 < St3) with St1 being the lowest and St3 the highest, which corresponded to the differential exposure to anthropogenic pressures, catchment characteristics, and hydrological flushing capacity. The concentration of all pollution sensitive parameters and the physicochemical baseline was found to be the lowest at station 1, near the Al-Kut/Baghdad checkpoint, which could indicate that the concentration of direct discharge inputs are being reduced or the overall dilution capacity is being increased. Stations 2 and 3, which are located in an urban infrastructure and residential area (Al-Ahdab Bridge), however, exhibited significantly higher variability and degradation, suggesting the accumulation of point and episodic pollution sources.

Water quality was progressive, worsening from autumn to spring. The hydrological conditions were stable and spatially uniform during the autumn period, while the conditions during the winter period were characterized by the presence of cumulative stressors associated with the reduction of river discharge, changes in mixing conditions and increased anthropogenic load (Pendleton et al., 2026). The most extreme degradation happened in spring when the season of thermal acceleration combined with seasonal runoff and release of accumulated pollutants. Hierarchical Clustering was used to confirm this, and it was found that temporal forcing is more important than the spatial differentiation, with samples grouping mainly by season, and not by station (Wu et al., 2024). This occurs as has been observed in regulated semi-arid river systems, where the flow regime is the most important factor in driving solute transport and pollutant retention, and seasonal climate cycles are also important.

4.2 Organic pollution and oxygen dynamics

An episodic rather than continuous loading regime characterizes the organic pollution regime in the study reach based upon the high COV for COD (114.4%) and BOD_5 (47.1%). The high positive correlation between BOD_5 and COD indicates that both measure biodegradable and total organic matter, and are presumably associated with discharge from domestic wastewater, agricultural runoff and urban stormwater. Organic loading showed clear seasonal variations, with low levels in autumn, and high levels in late winter and early spring. Mid-winter BOD_5 peaks reached up to 9 mg/L at Station 4 and COD levels were above 100 mg/L at all stations in May, indicating high levels of organic enrichment.

Thermal regimes and organic stress were closely related and tightly coupled with dissolved oxygen dynamics. The two mechanisms that were well established were reflected in the strong inverse relationship that was observed between DO and water temperature, and DO and organic indicators: decreased oxygen solubility with increased water temperature and increased microbial respiration with degradation of organic matter (Calvanese et al., 2024). The seasonal DO trajectory (high in the winter and low in the spring) reflects the temperature-related solubility limit, and the concurrent increases in organic pollutants further increase biochemically the demand for oxygen. These conditions approach thresholds for aerobic aquatic biota from ecological stress and especially during the spring season when high temperatures, high organic loads and low flushing rates coincide. It is interesting that DO is not associated with the mineral ion cluster, further emphasizing it as a biological response variable and not a geochemical constituent, which makes it an ideal indicator for early warnings of ecosystem health (Chen et al., 2025).

4.3 Mineralization and ionic composition

The ionic and mineral composition of the river water is cohesive and dominated by geochemical-anthropogenic fingerprint, which is evident from the strong inter-correlations (r = approximate 0.6–0.9) of EC, TDS, salinity, total hardness, Ca^{2+}, Mg^{2+}, Cl^{-} and SO_4^{2-}. It is a mineral cluster that is thought to be a result of a mineral concentration-dilution gradient rather than from any single pollution event, and is the result of seasonal hydrology. Higher concentrations in autumn and winter (EC: 1400–1800 µS/cm; TDS: 1000–1100 mg/L) are consistent with reduced flow volumes, increased evaporation and solute concentration during the semi-arid climatic period. The rapid decrease after March is related to higher runoff and hydrological flushing, which dilute the dissolved ions, even though the concentrations of other pollutants are rising.

This hydrochemical gradient was well accounted for by Principal Component Analysis (PC1, 51.6% variance) placing autumn samples in the positive half of the PC1 and spring samples in the negative half. Overall high to moderate ionic strength in the baseline seasonally indicates continued natural weathering of the basin lithology and agricultural drainage (sulfate and chloride salts) and domestic/industrial effluents. The low mineral concentrations in the non-treatment seasons do not indicate recovery to pristine concentrations, suggesting chronic loading of solutes. The results are in agreement with regulated rivers in arid and semi-arid regions where the evapotranspiration and low baseflow levels maintain high ionic loads even at high flow (Zeydalinejad, 2023).

4.4 Nutrient enrichment

The nutrient dynamics in the study reach is highly spatiotemporally heterogeneous and are decoupled from the dominant mineralization pathway. The relative variance (CV) values for phosphate (≈ 129%), nitrate (≈ 74%), showed that these were not steady state inputs but rather pulse driven ones. The overall moderate positive correlation between COD and PO_4^{3-} indicates that the carbon and phosphorus were enriched simultaneously, which is commonly linked to sewage discharges and agricultural runoff. Nitrate, however, showed weak to negative correlations with the cluster of mineral ions and positive correlations with phosphate and COD, suggesting a different transport pathway for nitrogen and phosphorus (N–P–C) possibly controlled by surface runoff and the intermittent addition of fertilizers.

Concentrations of nutrients rose significantly in spring, with NO_3^- concentrations in the range of 4-5 mg/L, and a high dispersion of phosphate. This is a seasonal increase that aligns with the cycles of agriculture, higher run off due to increased rainfall and lower capacity to dilute early in the flow regime. Enrichment with phosphorus is especially problematic in fresh water ecosystems where it is frequently limiting for primary production. High nutrient levels coupled with increasing temperatures and decreasing available DO during the spring season often support eutrophication, algal growth and hypoxia. Finally, the statistical separation of nutrients from the ionic cluster also suggests that management practices that focus on nutrient mineralization (such as salinity management) will not necessarily reduce the ecological risk of nutrients in a natural system, and specific nutrient abatement practices need to be implemented for agricultural and wastewater nutrient reductions (Srivastava et al., 2026).

4.5 WQI-based water-quality status

The Water Quality Index (WQI) integrates the data to show that the river condition was clearly worsening seasonally and had an obvious space-time trend. Water quality during the autumns ranged around 50, and interquartile ranges were relatively small, and this satisfied most beneficial uses. The mean WQI value increased to ~600–650 and variability ranges increased, reflecting increasing station heterogeneity, and winter conditions worsened significantly. The most critical time was in the spring as the mean WQI values were greater than 1300, and the highest values were greater than 2300 at Station 3, clearly making for poor to very poor conditions.

The very large error bars at Stations 2 and 3 are reflective of the episodicity of contamination and of the limited buffering capacity of the river system during low flow periods. The consistent spatial ranking (St3 > St2 > St4 > St1) for all months supports the concept of site-specific vulnerability, likely due to being near wastewater outfalls, urban drainage routes, and the low hydraulic residence time (Subudhi et al., 2025). The gradual progression over the season highlights the combined effect of water reduction, temperature rise and pollution input as all components of WQI. These results suggest that traditional static water-quality criteria may be a poor indicator of risk in transition periods from a management standpoint. Adaptive monitoring protocols along with seasonal flow augmentations and focused source control at high-WQI stations are needed to ensure the ecological function and water-use suitability (Alagulakshmi et al., 2025).

4.6 Multivariate interpretation

The multivariate framework adequately separates the many hydrochemical influences on water-quality variability in the Tigris River reach. A mineral/ionic enrichment group and an organic/nutrient loading group, both with an inverse relationship to DO, were identified by a Pearson correlation analysis. The separation was confirmed by Principal Component Analysis which accounted for 71.2% of the total variance (PC1: 51.6% and PC2: 19.6%): PC1 and PC2 were orthogonal hydrological and biogeochemical processes, respectively. The PCA biplot emphasized an overall seasonal shift in sample data, with high mineralization, low organic stress conditions in autumn, both, in winter and hydrological dilution of ions, with a concurrent increase in nutrient and organic stress conditions in spring.

Hierarchical clustering confirmed this, and showed a well-defined bifurcation between the spring samples and the autumn/winter samples, with seasonality as the major structuring factor. Euclidean distances for seasonal clusters are also low, which shows that regional hydroclimatic changes and biogeochemical processes related to temperature have more influence on the water-quality dynamics than localized spatial factors. A consistent dimensionality reduction across the different analyses for correlation, PCA and clustering confirms the statistical coherence of the analysis, in which ecologically relevant gradients are captured while noise is filtered out. These results offer a solid base for the analysis and prediction of future scenarios, the identification of sources, and adaptive management. Future research should combine land-use mapping with a hydrological flow record with sophisticated source tracking methods such as stable isotopes and positive matrix factorization to estimate the relative contribution of agricultural, domestic and industrial inputs, facilitating the precision interventions in relation to the identified seasonal and hydrochemical drivers (Ghavi Hossein-Zadeh, 2026).

5 .Conclusion

This research shows that water quality fluctuation in Tigris River at Al-Kut City is under a predictable seasonal cycle rather than being a spatial phenomenon. Pollution-sensitive parameters were found to have a high spatiotemporal variability, probably due to episodic anthropogenic inputs while baseline parameters are not significantly affected. A spatial gradient was observed, with good conditions at the upstream sites and poor conditions at the urban sites at the bottom of the flow. Water Quality Index continued to decrease from the fall to the spring period, related to the a) decrease of the hydrological flushing; b) temperature-dependent biogeochemistry processes; and c) accumulative organic load. Multivariate analyses showed that the system's variability is driven by the processes of seasonal hydrological forcing and independent pathways of organic–nutrient enrichment. The results suggest the spring season to be a vulnerable time of ecological stress and provide the basis for proactive management interventions that are seasonally adaptive. To secure the protection of freshwater resources, aquatic ecosystems and sustainable water governance in this semi-arid urban watershed, targeted monitoring, upgrading wastewater treatment infrastructure and appropriate flow regulation at highly impacted stations are crucial. Ongoing regulation and cooperation between stakeholders are still essential to facilitate environmental rehabilitation on a long-term basis.

References

Alagulakshmi, K., Arulraj, G. P., Gautam, S., & Joshi, S. K. (2025). Spatio-temporal patterns of land use and land cover, and their impact on groundwater quality in the industrialized Muvattupuzha basin. *Scientific Reports, 15*(1), 39189. https://doi.org/10.1038/s41598-025-24567-7

Calvanese, M., D'Angelo, C., Tutino, M. L., & Lauro, C. (2024). Whole-cell biosensor for iron monitoring as a potential tool for safeguarding biodiversity in polar marine environments. *Marine Drugs, 22*(7), 299. https://doi.org/10.3390/md22070299

Candraningtyas, C. F., Matin, H. H. A., & Ramadan, B. S. (2026). Microbiological contamination in a chemically safe river: Water quality assessment and mitigation framework for the Segah River. *IOP Conference Series: Earth and Environmental Science, 1586*, 012053. https://doi.org/10.1088/1755-1315/1586/1/012053

Chapman, D. (Ed.). (1996). *Water quality assessments: A guide to the use of biota, sediments and water in environmental monitoring* (2nd ed.). UNESCO/WHO/UNEP.

Chen, Q., Tang, K., Zhai, W., Zhu, Z., Yang, J. Y. T., He, Z., Li, M., Kao, S. J., Yang, J., Zheng, Q., Lønborg, C., Thomas, H., & Jiao, N. (2025). Microbial responses to ocean deoxygenation: Revisiting the impacts on organic carbon cycling. *iScience, 28*(7), 112826. https://doi.org/10.1016/j.isci.2025.112826

Fernandes, L. S. (2023). A framework model to integrate sources and pathways in the assessment of river water pollution. *Journal of Environmental Management, 340*, 117900. https://doi.org/10.1016/j.envpol.2024.123661

Ghavi Hossein-Zadeh, N. (2026). Advancing climate-resilient livestock systems: Next-generation emission mitigation strategies and integrated technological innovations. *Veterinary and Animal Science, 31*, 100588. https://doi.org/10.1016/j.vas.2026.100588

Ighalo, J. O., & Adeniyi, A. G. (2021). A comprehensive review of water quality monitoring and assessment in Nigeria. *Water Practice and Technology, 16*(2), 305–325. https://doi.org/10.1016/j.chemosphere.2020.127569

Kuchangi, S. N., Mruthunjayappa, M. H., & Kotrappanavar, N. S. (2023). An overview of water pollutants in present scenario. *Environmental Pollution and Protection, 6*(1), 101–112. https://doi.org/10.1016/B978-0-323-99861-1.00001-1

Paruch, A. M., & Mæhlum, T. (2012). Specific features of *Escherichia coli* and coliform bacteria as indicators of fecal contamination in surface water. *Water Research, 46*(1), 173–182.

Pendleton, A., Wells, M., & Schmidt, M. L. (2026). Upwelling periodically disturbs the ecological assembly of microbial communities in Lake Ontario. *ISME Communications, 6*(1), ycag023. https://doi.org/10.1093/ismeco/ycag023

Srivastava, S., Mir, R. A., Hussain, S. J., Mitra, S., Srivastava, S., Kumar, P., & Kaur, H. (2026). Microbial engineering for pesticide degradation: Current insights and future directions for sustainable agriculture. *Frontiers in Microbiology, 17*, 1751932. https://doi.org/10.3389/fmicb.2026.1751932

Subudhi, S., Pati, A. K., Bose, S., Sahoo, S., Pattanaik, A., Acharya, B. M., & Thakur, R. R. (2025). Prediction of groundwater quality assessment by integrating boosted learning with DE optimizer. *Scientific Reports, 16*(1), 618. https://doi.org/10.1038/s41598-025-30122-1

Wetzel, R. G. (2001). *Limnology: Lake and river ecosystems* (3rd ed.). Academic Press.

Wu, Y., Yin, X., Zhou, G., Bruijnzeel, L. A., Dai, A., Wang, F., Gentine, P., Zhang, G., Song, Y., & Zhou, D. (2024). Rising rainfall intensity induces spatially divergent hydrological changes within a large river basin. *Nature Communications, 15*(1), 823. https://doi.org/10.1038/s41467-023-44562-8

Zeydalinejad, N. (2023). An overview of the methods for evaluating the resilience of groundwater systems. *MethodsX, 10*, 102134. https://doi.org/10.1016/j.mex.2023.102134